Available online at www.sciencedirect.com
SCIENCE DIRECT
Catalysis Today 105 (2005) 414–420
CATALYSIS TODAY
www.elsevier.com/locate/cattod

Modelling of reactive stripping in monolith reactors

Tilman J. Schildhauer [a,*], Sander Tromp [a], Ivo Müller [b], Alexej Schilkin [b], Eugeny Y. Kenig [b], Freek Kapteijn [a], Jacob A. Moulijn [a]

[a] *Technical University Delft, DelftChemTech, Reactor and Catalysis Engineering Julianalaan 136, NL-2628 BL Delft, The Netherlands*
[b] *University of Dortmund, Department of Biochemical and Chemical Engineering Emil-Figge-Str. 70, 44221 Dortmund, Germany*

Abstract

In this work, (reactive) stripping carried out in film flow monolith reactors developed for counter-current operation is investigated. Usually mass transfer in reactive separation has to be determined experimentally due to the complex flow patterns. However, monoliths have a simple geometry; only laminar flow is present throughout the column. This allows the calculation of the thickness of the liquid layer directly using Navier–Stokes equations. With this thickness known, the mass transfer can be calculated based on the convection in axial direction, diffusion in radial direction and vapour–liquid equilibrium. A model has been developed and implemented in Fortran® based on the concept of a direct solution of convective diffusion equations, using the Thomas algorithm for solving the counter-current operation mode. Experimental data from literature have been used to validate the model for a binary and a multi-component system. The stripping of oxygen from saturated water by nitrogen was modelled assuming Fickian diffusion and vapour–liquid transfer based on the Henry constants. In a second step, multi-component diffusion and complex mass transfer at the interface were taken into account to describe the stripping of water by nitrogen from a mixture of hexyl-octanoate and cumene (solvent) under reactive stripping conditions.

Keywords: Monolith reactors; Modelling; Film flow; Reactive stripping; Thomas algorithm

1. Introduction

Reactive distillation and reactive stripping are typical examples of integrated chemical processes where more than one functionality is integrated in one apparatus [1]. As both processes are a combination of reaction and gas–liquid separation, they are preferably operated counter-currently. Therefore, structured catalyst supports have been developed for these processes, which combine high gas–liquid mass transfer with low pressure drop and high flooding limits.

Under these structured catalyst supports, reactive distillation packings like Sulzer Katapak-S®, -SP® or Montz Multipak® are well known and have been investigated extensively. Recently, special types of monoliths with wide channels have been developed [2] which allow for a laminar liquid film flowing down along the catalytically coated walls, where the reaction takes place (see Fig. 1). In the channel core, a counter-current flow of permanent (inert) gas can strip compounds from the liquid phase to shift the equilibrium or avoid inhibition of the catalyst activity by strong adsorption of a (by-)product. The feasibility of applying these film flow monoliths for reactive stripping in pilot scale has been demonstrated successfully [3].

For the film flow monoliths, several channel geometries are available which differ not only in geometric surface area and hydraulic diameter but also in their wetting patterns. As shown in Fig. 2, predominantly corner flow can be observed for the square channel whereas a bigger part of the wall is irrigated in internally finned monoliths (IFM). Monoliths with strongly rounded channel corners (MRC) achieve the best distribution of the liquid; the film thickness is quite constant and the walls are nearly completely wetted. It has been found that these specific wetting patterns cause also differences in the residence time distribution (RTD) and mass transfer [1].

* Corresponding author at: Laboratory for Energy and Material Cycles, Paul-Scherrer-Institut, CH-5232 Villigen PSI, Switzerland.
Tel.: +41 56 310 27 06; fax: +41 56 310 21 99.
E-mail address: tilman.schildhauer@psi.ch (T.J. Schildhauer).

0920-5861/$ – see front matter © 2005 Elsevier B.V. All rights reserved.
doi:10.1016/j.cattod.2005.06.052

Nomenclature

A_{rad}	cross sectional area in radial direction (m^2)
C	concentration (mol/m^3)
d_{film}	film thickness (m)
D	diffusion coefficient (m^2/s)
g	gravitational constant (m/s^2)
k_G	equilibrium constant
k_La	mass transfer coefficient (s^{-1})
L	total length of a channel (m)
r	radius at a certain location in the column (m)
r_i	reaction rate (mol/s)
r_{film}	radius of the interface between the gas and the liquid (m)
R	total radius of a channel (m)
u_z	axial velocity (m/s)
w_0	superficial velocity (m/s)
x	molar fraction in liquid phase
y	molar fraction in gas phase
z	height at a certain location in the column (m)

Greek letters

μ_L	liquid viscosity (Ns/m^2)
ρ_L	liquid density (kg/m^3)
$\Phi_{V,L}$	liquid flow rate (m^3/s)

The modelling of catalyst supports for gas–liquid processes has been widely investigated [4–6]. However, as the exact position of the gas–liquid interface and the flow patterns in both phases are hard to predict, usually the two film approach is chosen to describe the mass and heat transfer [7]. In this approach, both gas and liquid phase are assumed to be completely mixed and separated by apparent laminar films on both sides of the gas–liquid interface comprising the complete mass or heat transfer resistance. The area of the interface and thickness of the apparent films in this approach then have to be determined by sets of mass transfer experiments [8].

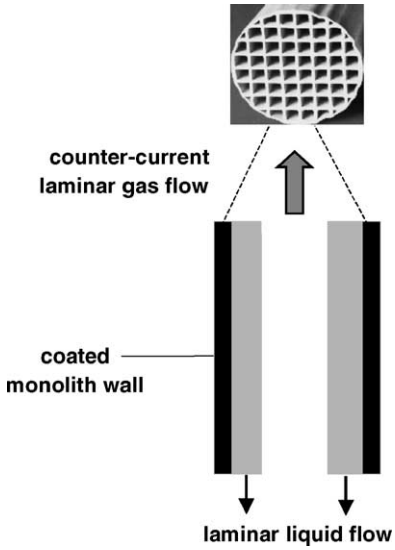

Fig. 1. Schematic representation of a film-flow-monolith.

In the case of film flow monoliths, the situation is less complex. As laminar flow is predominant, film thicknesses and velocity profiles can be calculated immediately [9]. In the case of strongly rounded channel geometry (MRC), the problem can even be simplified to a two-dimensional system under the assumption of constant film thickness around the circumference.

In this work, it is attempted to directly model reactive stripping under counter-current operation in film flow monoliths with strongly rounded channel walls. Experimental data obtained with MRC monoliths are used to validate the model.

2. Approach

As mentioned in the introduction, film flow monoliths are characterised by laminar flow. This is also found in RTD experiments. Fig. 3 shows the dimensionless RTD which is obtained theoretically as answer of a fully laminar flow for an ideal Dirac-peak and the RTD of a finned monolith (IFM) of 75 cm length (from [2]). Typical for both figures are the high peaks at times earlier than the mean residence time and the very long tailing. Both phenomena can be explained with the character of laminar flow. The fastest liquid can be found at the film surface in the corners, as here the distance to the channel wall is maximal. In the theoretical laminar system with parabolic velocity profile, the maximum velocity is double the average velocity. Therefore breakthrough is expected around $\theta = 0.5$, whereas the tailing represents the liquid flowing with very small velocity next to the wall. In round channel geometries, the breakthrough comes later than in square geometries, because the maximum film thickness is lower. However, as the channel wall is nearly completely wetted in round geometries, the tailing increases.

Based on the assumption of fully developed laminar flow and constant film thickness, the velocity profile in the liquid can be calculated from a balance of drag forces and gravitational force with a no-slip boundary at the wall and a full slip boundary at the interface. Plug flow is assumed for the gas phase. The complete situation is sketched in Fig. 4.

The radial profile of the axial velocity can be calculated by the following equation derived from the Navier–Stokes equations:

$$u_z = -\frac{\rho_L g}{2\mu_L}\left(\frac{1}{2}r^2 - r_{film}^2\ln(r) + r_{film}^2\ln(R) - \frac{1}{2}R^2\right) \quad (1)$$

The film thickness can be found by using the expression for the liquid flow rate and by integrating the axial velocity

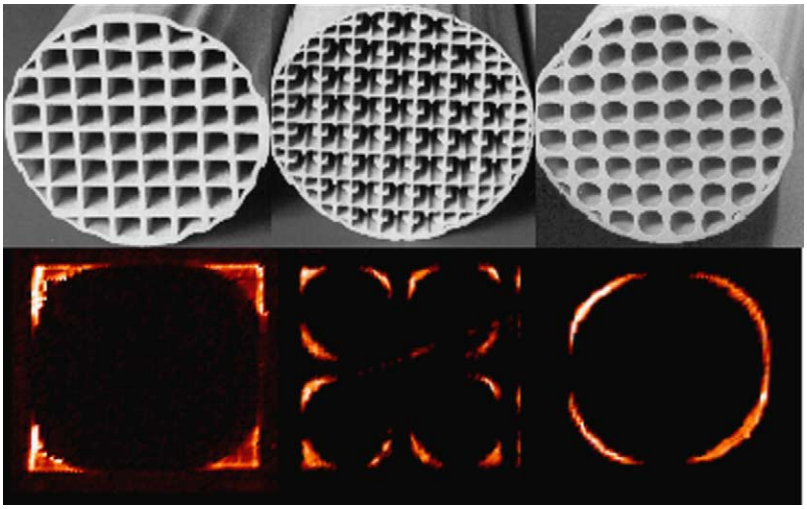

Fig. 2. Film flow monoliths and MRI-representation of the liquid distribution in one channel: squared channels left, internally finned (IFM) middle, rounded corners (MRC) right.

profile over the radius and azimuthal co-ordinate:

$$\Phi_{\mathrm{V,L}} = -\frac{\rho_{\mathrm{L}} g \pi}{2\mu_{\mathrm{L}}}\left(R^2 r_{\mathrm{film}}^2 + r_{\mathrm{film}}^4 \ln(r_{\mathrm{film}}) - \frac{1}{4}R^4 - \frac{3}{4}r_{\mathrm{film}}^4 - r_{\mathrm{film}}^4 \ln(R)\right) \tag{2}$$

Furthermore, the model considers axial convection as well as radial diffusion in both phases, but no axial diffusion. At the gas–liquid interface, equilibrium state is assumed. Reaction is taken into account at the catalytically coated wall. Therefore, the mass transfer model consists of the following equation:

$$u_z \frac{\partial C}{\partial z} = D \frac{1}{r}\frac{\partial}{\partial r}\left(r \frac{\partial C}{\partial r}\right) \tag{3}$$

where u_z is given by Eq. (1).

To solve this partial differential equation for both phases, the inlet concentrations for both phases should be known.

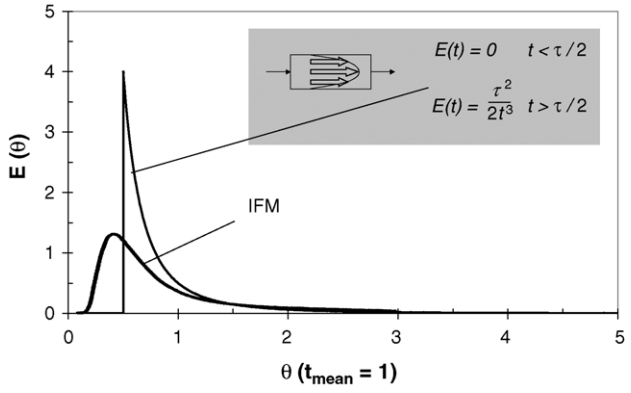

Fig. 3. Dimensionless RTD for laminar tube flow and an internally finned film-flow monolith (IFM).

Further, the following boundary conditions are necessary:

$$\text{at} \quad r = R, \quad A_{\mathrm{rad}} D_i \frac{\partial C}{\partial r} = -r_i \tag{4}$$

$$\text{at} \quad r = 0, \quad \frac{\partial c}{\partial r} = 0 \tag{5}$$

$$\text{at} \quad r = r_{\mathrm{film}}, \quad \left(A_{\mathrm{rad}} D \frac{\partial C}{\partial r}\right)_{\mathrm{gas}} = \left(A_{\mathrm{rad}} D \frac{\partial C}{\partial r}\right)_{\mathrm{liquid}} \tag{6}$$

$$\text{at} \quad r = R, \quad y = k_{\mathrm{G}} x \tag{7}$$

For the solution of the problem, the complete system was discretised using a fully implicite scheme and all equations were rewritten as finite difference equations. These equations are solved by the Thomas algorithm [10]. The solution method is similar to that suggested in [11]. When using the Thomas algorithm for a two-phase system, initial estimates of the concentrations at the interface need to be given, and the solution is obtained iteratively. Especially for the simula-

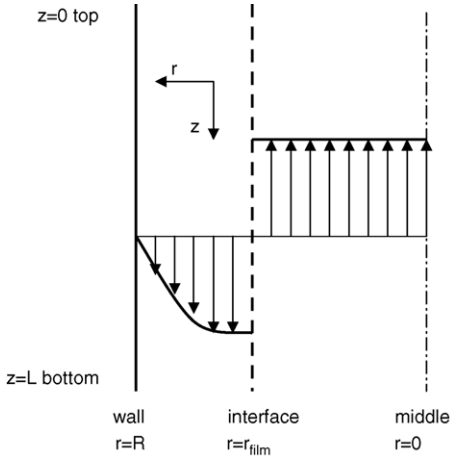

Fig. 4. Velocity profile and reference frame.

tion of counter-current operation, the Thomas algorithm is considered as advantageous because of its robustness.

3. Results

In a first step, simple mass transfer from the liquid phase to the gas phase without reaction was considered. As experimental data on stripping of oxygen from saturated water by nitrogen in film flow monoliths (MRC) at ambient conditions was available [1], this system was chosen as model system for the validation of the binary model. As the concentration of oxygen in both phases is very small, Fickian diffusion and the Henry constant for the equilibrium description can be applied.

Fig. 5 shows the simulated axial profile of averaged oxygen concentrations in both phases for co-current operation (superficial liquid velocity $u_S = 1.6$ cm/s). The input parameters are given in Table 1. It is found that the stripping performance is best immediately after the inlet.

From the calculated radial oxygen profiles in the liquid phase (Fig. 6), it becomes obvious, that this system is completely diffusion-limited. Any oxygen reaching the interface is transferred immediately to the gas phase. Therefore, mass transfer is highest immediately behind the inlet before the radial concentration profile has completely developed. Liquid film thickness has the biggest impact on the mass transfer. As a consequence of the diffusion limitation, the variation of the gas velocity has no influence on the mass transfer, when the gas flow is beyond a certain minimum. Above a certain minimum liquid flow, no difference for co- or counter-current operation is found in the simulations. Below this minimum, the liquid film is very thin, so that the transport is not longer limited by the diffusion and the equilibrium limitation starts playing a role.

From these data, the k_La value can be calculated according to the approach of [9] for the region where profiles are completely developed:

$$k_La = \frac{w_0}{L} \ln\left(\frac{c_{in}}{c_{out}}\right) \quad (8)$$

The value for k_La found in the simulation is 0.0195 s^{-1} compared to 0.0185 s^{-1} from the literature [1]. A slightly higher value from the simulations was expected due to the non-idealities in the experiments, especially due to incomplete wetting in MRC monoliths, which limits the mass transfer.

To understand the influence of varying film thicknesses, a comparison was done between the mass transfer in two channels with a thick and thin film, respectively, on the one hand, and two channels with the same film thickness and the same overall liquid flow, on the other hand (see Table 2). A deviation of the two films of about plus and minus 20% from the constant film thickness for an averaged flow leads to a decrease in mass transfer of about 1.5%. Even a severe deviation from the averaged flow constant film thickness of

Table 1
Parameters for the simulation of the simple system

Parameter	Amount
Liquid density (kg/m^3)	1000.0
Gas density (kg/m^3)	1.3
Liquid diffusion coefficient (m^2/s)	1.67×10^{-9}
Gas diffusion coefficient (m^2/s)	2.0×10^{9}
Liquid viscosity (Pa s)	1.002×10^{-3}
Henry coefficient	3.99×10^{4}
Channel radius (m)	2.155×10^{-3}
Length of the column (m)	0.5
Number of channels in the monolith	44
Total gas concentration (mol/m^3)	44.6
Total liquid concentration (mol/m^3)	56000
Linear liquid velocity (m/s)	0.02
Entrance molar fraction	5.23×10^{-6}
Number of discretes in radial direction (liquid)	300
Number of discretes in radial direction (gas)	300
Number of discretes in axial direction	600

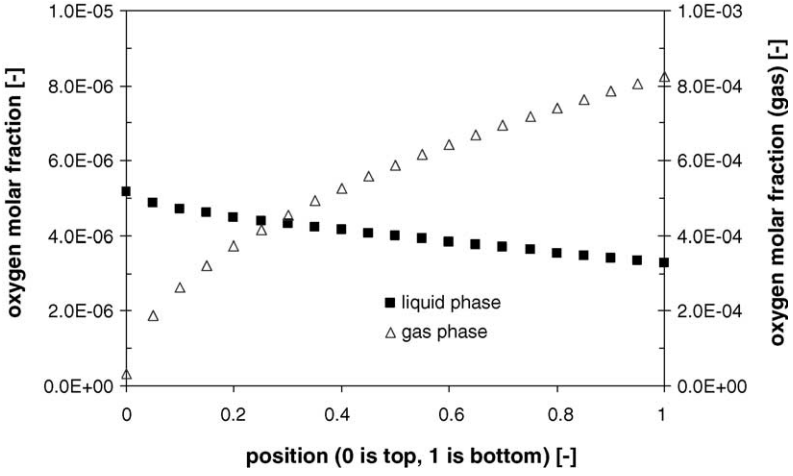

Fig. 5. Axial average concentration profile of oxygen (input in Table 1).

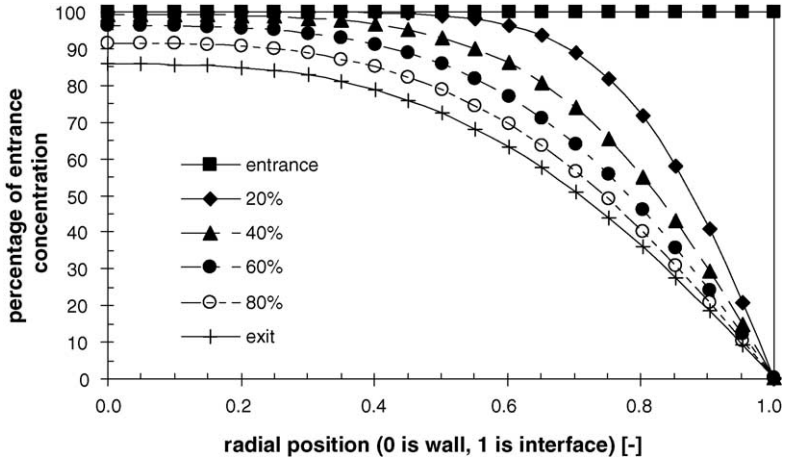

Fig. 6. Radial concentration profile of oxygen in the liquid at different axial positions (input in Table 1); calculated film thickness 0.22 mm.

Table 2
Comparison of two channels with constant film thickness and two channels with different film thicknesses, but same total liquid flow rate

	Deviation of film thickness d_{film} (%)	d_{film} in channels with constant d_{film} (base case)	d_{film} in channel with smaller i_{film}	d_{film} in channel with higher d_{film}	Deviation in stripping performance(%)
Case 1	ca. 20	0.260	0.20	0.30	−1.5
Case 2	ca. 40	0.285	0.15	0.35	−5.2

plus 40% in one channel and minus 40% in the other channel reduced the mass transfer by not more than 5.2%. Therefore, deviations in the film thickness have a minor impact in the case of diffusion limited mass transfer and are negligible in systems, where the equilibrium is dominating. From these findings, it was concluded, that the model can be considered as validated for the simple system without reaction.

In the next step, a multi-component system was chosen. From the experiments on reactive stripping in pilot scale [3], data for the stripping of water by nitrogen from a mixture of solvent (cumene), octyl-hexanoate ester and traces of octanol-1 and hexanoic acid at 5 bar_{abs} and 160 °C were available. Due to the high mass transfer rates of water as well as cumene, binary diffusion coefficients or Henry constants can no longer be applied. It was therefore necessary to determine effective diffusion coefficients and complex equilibrium data with Aspen Plus®.

Fig. 7 shows the radial water concentration profiles in the organic liquid phase for different axial positions. The input parameters for this simulation are given in Table 3. The nearly flat profiles indicate that this system is dominated by the equilibrium. The water diffuses fast through the liquid phase, but the phase transition is limiting. Therefore, the determination of the equilibrium constant k_G for water in this system by Aspen Plus® and its validation with experimental data was essential.

With the validated k_G, stripping of water from the ester/cumene mixture at 160 °C, 5 bar_{abs} was simulated for different

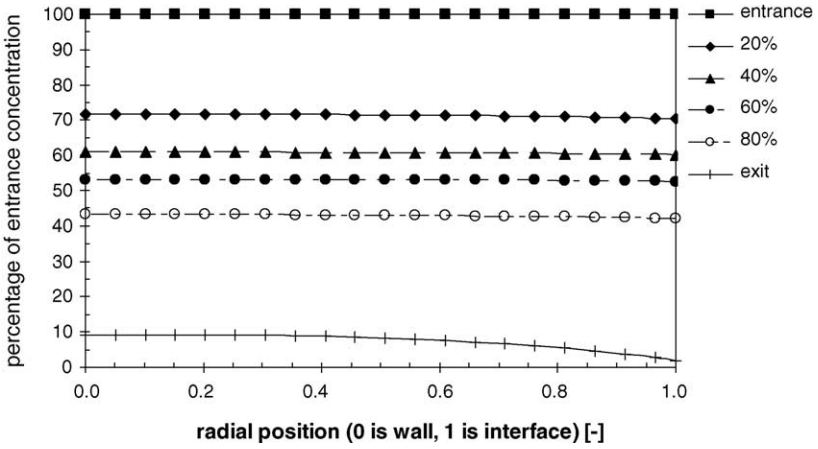

Fig. 7. Radial liquid concentration profile of water in multi-component stripping experiments (160 °C, 4 barg, other input can be found in Table 3); calculated film thickness 0.12 mm.

Table 3
Parameters for the simulation of the multi-component system

Parameter	Amount
Channel radius (m)	2.155×10^{-3}
Column length (m)	2
Number of channels	44
VLE constant water	9.39
Liquid diffusion coefficient water (m^2/s)	2.29×10^{-8}
Gas diffusion coefficient water (m^2/s)	6.65×10^{-6}
Liquid density (kg/m^3)	777
Liquid viscosity (Pa s)	2.789×10^{-4}
Gas density (kg/m^3)	6.775
Total gas concentration (mol/m^3)	140.5
Total liquid concentration (mol/m^3)	5770
liquid flow rate (kg/h)	25
Entrance molar fraction water	1.49×10^{-2}
Number of discretes in radial direction (liquid)	700
Number of discretes in radial direction (gas)	100
Number of discretes in axial direction	200

gas flows. Fig. 8 shows a comparison between experiments and simulations. It is obvious that due to the equilibrium constraints, the stripping performance increases with the gas flow in counter-current operation whereas equilibrium is reached in co-current operation. The results of the simulation are in very good agreement with the experiments. Only for the counter-current operation with the highest gas velocity of 500 Nl/h, the model predicts a higher stripping performance. This might be caused by an overprediction of the water diffusion coefficient by Aspen Plus®.

With the validated model, some parameter variations were carried out to better understand the sensitivity of the system. Fig. 9 shows the axial profile of the radially averaged water concentration in the liquid. For a counter-current nitrogen flow of 500 Nl/h, high mass transfer (i.e. high concentration gradients) is observed at the top and the bottom of the column. The same is found in Fig. 7. At the inlet, the high mass transfer is caused by high water concentrations meeting not yet

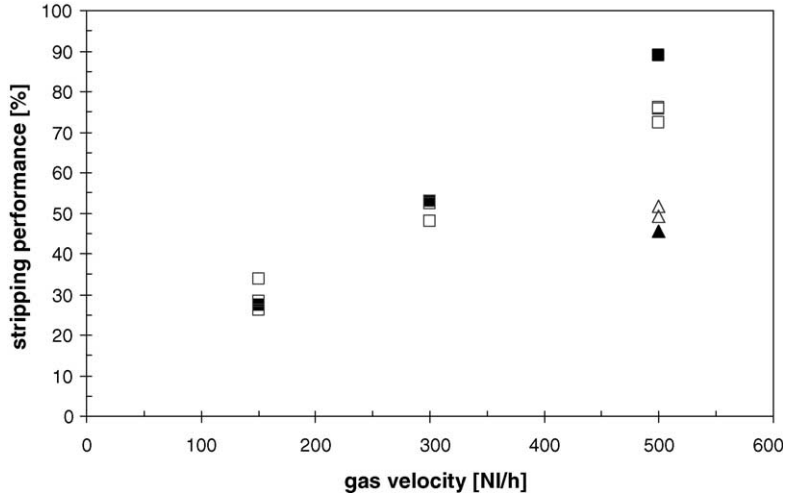

Fig. 8. Comparison of experiments and simulations for multi-component stripping (160 °C, 4 barg, other input can be found in Table 3): filled symbols model, open symbols experiments; squares counter-current, triangles co-current.

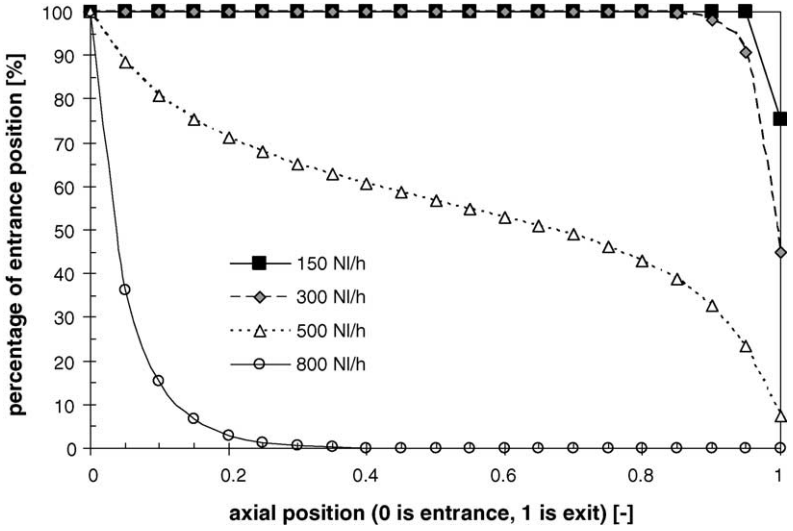

Fig. 9. Average liquid concentration profile of water for different gas flows (liquid flow 25 kg/h, 160 °C, 4 barg).

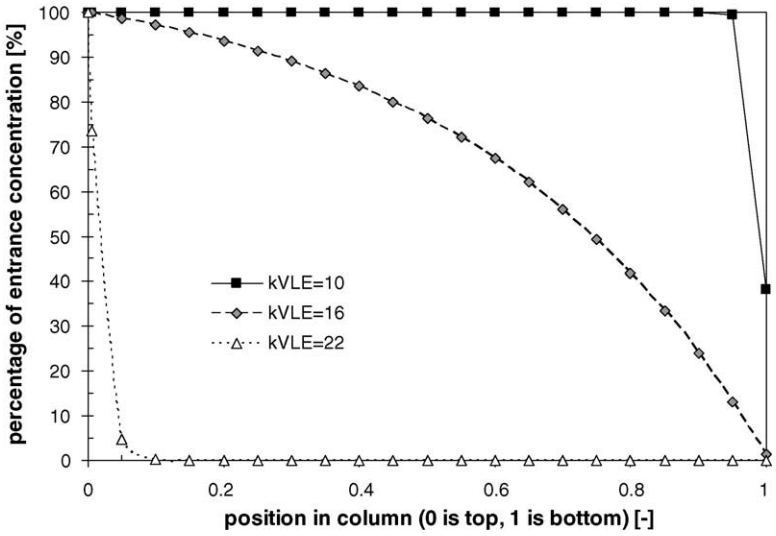

Fig. 10. Effect of k_G on the liquid stripping position (gas flow 500 Nl/h, 160 °C, 4 barg, other input as in Table 3).

completely saturated nitrogen. At the liquid outlet, the last rests of water can be stripped by the entering pure nitrogen. However, if the nitrogen flow is decreased, the gas phase will be saturated and stripping takes place only at the gas inlet at the bottom of the column.

Fig. 10 shows the effect of varying the value of the equilibrium constant of water k_G. Depending on its value, the position of the stripping can be very different for given flow rates, film thickness and concentrations. This can have a strong impact for the reaction which would take place in the column. In the shown example, the water concentrations at the catalyst and therefore the catalyst activity and the maximally obtainable (equilibrium) conversion will differ strongly. This emphasizes the importance of modelling and simulation in the design of separation processes.

4. Conclusions

Counter-current stripping carried out in film flow monolith reactors was investigated by modelling and simulation. The thickness of the laminar film in these monoliths was calculated directly using Navier–Stokes equations. This allowed calculating the gas–liquid mass transfer based on the convection in axial direction, diffusion in radial direction and vapour–liquid equilibrium for a simple and a multi-component system. The model was implemented in Fortran® based on the concept of a direct solution of convective diffusion equations, using the Thomas algorithm for solving the counter-current operation mode. Experimental data from literature have been used to succesfully validate the model for both systems. The stripping of oxygen from saturated water by nitrogen could be described assuming Fickian diffusion and gas–liquid transfer based on the Henry constants. With multi-component diffusion coefficients and complex equilibrium constants, both determined by Aspen Plus®, the stripping of water by nitrogen from a mixture of hexyl-octanoate, cumene (solvent) and traces of hexanoic acid and octanol-1 could be predicted under reactive stripping conditions. Variations of input parameters showed that the stripping performance might change strongly on even moderate changes of e.g. the gas flow or the equilibrium constant for the compound to be stripped. This emphasizes the importance of modelling and simulation in the design of reactive separations.

Acknowledgement

Valuable discussions with Markus Klöker are gratefully acknowledged.

Reference

[1] T.J. Schildhauer, A.K. Heibel, A. Yawalkar, F. Kapteijn, J.A. Moulijn, Reactive stripping in structured catalytic reactors—hydrodynamics and reaction performance, in: K. Sundmacher, A. Seidel-Morgenstern, A. Kienle (Eds.), Integrated Chemical Processes, Wiley-VCH, March 2005.
[2] P.J.M. Lebens, Development and design of a monolith reactor for gas–liquid countercurrent operation, Ph.D. thesis, TU Delft, 1999.
[3] T.J. Schildhauer, F. Kapteijn, J.A. Moulijn, Chem. Eng. Proc. 44 (2005) 695–699.
[4] J.R. Fair, A.F. Seibert, M. Behrens, P.P. Saraber, Z. Olujic, Ind. Eng. Chem. Res. 39 (2000) 1788.
[5] J.M. van Baten, R. Krishna, Chem. Eng. Sci. 57 (2002) 1531.
[6] M. Klöker, E.Y. Kenig, A. Górak, Catal. Today 79–80 (2003) 479.
[7] K. Lewis, W.G. Whitman, Ind. Eng. Chem. 16 (1924) 1215.
[8] A. Kolodziej, M. Jaroszyski, A. Hoffmann, A. Górak, Catal. Today 69 (2001) 75.
[9] A.K. Heibel, T.W.J. Scheenen, J.J. Heiszwolf, H. Van As, F. Kapteijn, J.A. Moulijn, Chem. Eng. Sci. 56 (2001) 5935.
[10] G.H. Bruce, D.W. Peaceman, H.H. Rachford, J.D. Rice, Trans. Am. Inst. Min. Engrs (Petrol Div.) 198 (1953) 79.
[11] E.Y. Kenig, L.P. Kholpanov, J. Eng. Phys. 59 (1990) 896.